IL NUOVO CIMENTO Vol. 30 C, N. 1 Gennaio-Febbraio 2007
DOI 10.1393/ncc/i2006-10041-y

Non-destructive characterisation of a Villanovan sword using time-of-flight neutron diffraction(*)

L. Bartoli(1), S. Siano(1)(**), W. Kockelmann(2), J. Santisteban(2), M. Miccio(3) and G. De Marinis(4)

(1) *IFAC-CNR - via Madonna del Piano, I-50019 Sesto Fiorentino, Italy*
(2) *Rutherford Appleton Laboratory, ISIS Facility - Chilton, OX11 0QX, UK*
(3) *Soprintendenza per i Beni Archeologici della Toscana - Largo il Boschetto 3 50100, Firenze, Italy*
(4) *Soprintendenza per i Beni Archeologici delle Marche - via Birarelli 18 60121, Ancona, Italy*

(ricevuto il 31 Ottobre 2006; pubblicato online il 9 Febbraio 2007)

Summary. — In the present work we report an example application of time-of-flight neutron diffraction for the non-destructive characterisation of ancient bronzes. A Villanovan sword tightly joined to its scabbard by corrosion has been investigated. Data on alloy composition of the different parts and information about the manufacturing techniques have been successfully achieved. The present study is part of an extensive non-destructive investigation program concerning bronze productions of Central Italy during the Iron Age.

PACS 61.12.-q – Neutron diffraction and scattering.
PACS 81.05.Bx – Metals, semimetals, and alloys.
PACS 81.70.-q – Methods of materials testing and analysis.

1. – Introduction

In the last years time-of-flight neutron diffraction (TOF-ND) has been proposed for non-destructive characterisation of archaeological materials such as ceramics [1, 2], metals [3-8] and marbles [9]. These experiments have clearly demonstrated the potential of the approach associated with the high signal-to-noise ratio and with a reliable statistics of the acquired diffraction patterns. On the other hand, the low spatial and analytical resolution due to the low fluxes and the low scattering coefficients makes neutron diffraction unsuitable for stratigraphic and traces analyses. TOF-ND has been proven

(*) Paper presented at the Workshop "RICH—Research Infrastructures for Cultural Heritage", Trieste, December 12-13, 2005.
(**) E-mail: s.siano@ifac.cnr.it

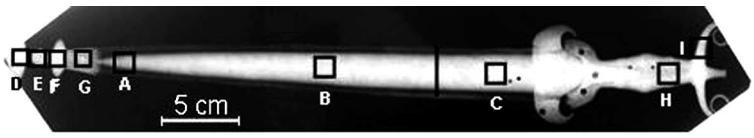

Fig. 1. – Radiography of the sword showing the nine different analysed sites (A-I). The line in the middle represents the cross-section which has been scanned to obtain a map of intensity, lattice parameter and peak width.

as the most suitable tool to achieve quantitative metallurgical data on alloy and mineral phase contents, preferred orientation distribution of crystallites and residual stresses produced by cold working in a non-destructive way [3-6]. Here a Villanovan sword from the Marches National Museum of Archaeology, (Ancona, Italy) was thoroughly investigated. The artefact is particularly interesting for its complexity as well as because conventional approaches could not allow analysing composition and microstructure of the blade, which is joined with the scabbard by corrosion processes. Information about the different alloy compositions and the manufacturing techniques were provided by quantitative multiphase analysis and 2D mapping of scattering intensity, peak width and microstrain on a cross-section of the sword. This latter technique, reported here for the first time, broadens the potential of the TOF-ND approach.

2. – Materials and methods

The artefact is a Villanovan (phase II) antennas-type sword dated II half of the VIII century B.C., which was found in Fermo (Ascoli Piceno, Italy) in 1957. On the basis of visual examination and radiography (fig. 1) various interesting zones have been selected (A-I) where possible differences in composition and alloy processing could be found. At least 6 different pieces mounted together are recognisable starting from the left of fig. 1: scabbard tip, blade, scabbard, manufactured with metal sheets, mouth, handle with decorative "antennas".

Several measurements were carried out in different zones. A-C) along the blade to evidence possible differences of hardening degree. D-G) on the tip because it was unclear whether it was crafted by a single casting or by mounting together two different pieces. H-I) on the handle to point out differences both in working process and in composition. A 2D scan of a cross-section was performed in the zone indicated by the black line to obtain a map of intensity, lattice parameter and peak width distributions of the entire section. The measurements were carried out at the pulsed neutron source ISIS (Rutherford Appleton Laboratory, UK) on two different instruments. Diffraction measurements on sites A-I were performed on ROTAX [1,2], a medium resolution powder diffractometer covering a d-spacing range of 0.3–20 Å. The neutron spot sizes were 1.5×1.5 cm^2. The quantitative multiphase analysis was performed using the GSAS code [10] through Rietveld refinement of the diffraction patterns. The relative peak broadening ($\Delta d/d$) was derived through a Gaussian fitting of the (200) α(Cu) reflection peak. The mapping of the peak intensities, lattice parameters and peak widths was instead performed on ENGIN-X [11], a high spatial resolution scanning diffractometer especially designed for investigating residual stresses in mechanical components. The instrument is equipped with two detector banks, which collect neutron scattered in the orthogonal direction with respect to the incident beam axis. A slit and two long collimation windows provide a relatively high spatial

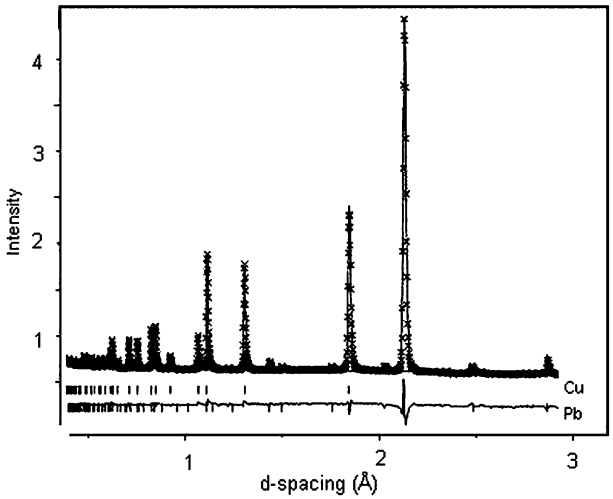

Fig. 2. – Example of pattern refinement of site A of the sword. Crosses represent the observed pattern, the continuous line is the Rietveld refinement and the line at the bottom shows the difference between the two.

selectivity. In the present case the gauge volume of the scanning was $1 \times 1 \times 13$ mm^3, with the longest side along the sword longitudinal axis.

3. – Results

3˙1. *Phase analysis*. – The acquired *d*-spacing patterns were dominated by the alloy peaks belonging to a copper-type face-centered cubic structure (fig. 2) with lower intensity lead and cuprite peaks in some probed zones.

As well known, the presence of a separated lead phase in leaded bronzes is due to its immiscibility at the solid state with copper [12]. The patterns were analysed through multi-bank Rietveld refinement, taking into account possible texture effects. The composition results are summarized in table I. The chemical composition of the bronze was achieved in three steps: 1) The refinement provides the weight fraction of the three phases here involved (binary alloy, lead, cuprite) and the respective lattice parameters. 2) The metal phases are re-normalised to 100%, whereas the content of cuprite in table I is the absolute one directly derived by Rietveld refinement. 3) Copper and tin contents of the binary alloy are achieved by exploiting the linear dependence of bronze lattice parameter on tin content (Vegard law) experimentally determined in previous works [3, 4].

The blade and the handle are ternary bronze alloys with different compositions. The higher tin content of the former (12–13 wt%) is consistent with the requirement of a higher hardness of the blade. In the decorative tip lead was detected only in the zones D and F in a very low content (1 wt%).

3˙2. *Peak shape analysis*. – As mentioned above, peak shape analysis can provide qualitative information about the metal microstructure and therefore metal processing. As-cast alloys are characterised by broad and irregular diffraction peaks due to dendritic segregation, whereas annealing and recrystallization processes produce narrow peaks. Annealing followed by cold working gives rise to an intermediate peak width, depending

TABLE I. – *Phase quantification and alloy composition derived from the Rietveld refinement of the TOF-ND patterns.*

Site	Cu (wt%)	Sn (wt%)	Pb (wt%)	Cu_2O (wt%)
A	83.0	12.9	4.1	/
B	82.1	11.9	6.0	/
C	82.8	11.7	5.5	/
D	88.1	10.8	1.1	2.1
E	90.4	9.6	/	/
F	88.1	10.8	1.1	2.1
G	89.1	10.9	/	1.4
H	90.7	7.0	2.3	/
I	91.2	7.1	1.7	/

on the residual stress values and distributions [4, 6]. Figure 3 shows the comparison among the (200) α(Cu) peaks associated with the different probed zones. The (200) peak was selected because it is intense and isolated from other reflections: in particular, it is not superimposed to the δ(Cu) phase, which can appear at high tin contents.

All of the probed zones of the scabbard decorative termination (D, E, F, G) exhibited broad and structured peaks, which indicates that this piece was produced by casting and likely mechanically polished. A very similar shape and broadening is provided by the central part of the handle (site H) whereas a very narrow and smooth peak is associated with the final part of the handle itself (site I, "antennas"), which demonstrates it underwent a hardening and annealing cycle. This result is very interesting because it shows that, although the handle and the antennas have the same composition, they were

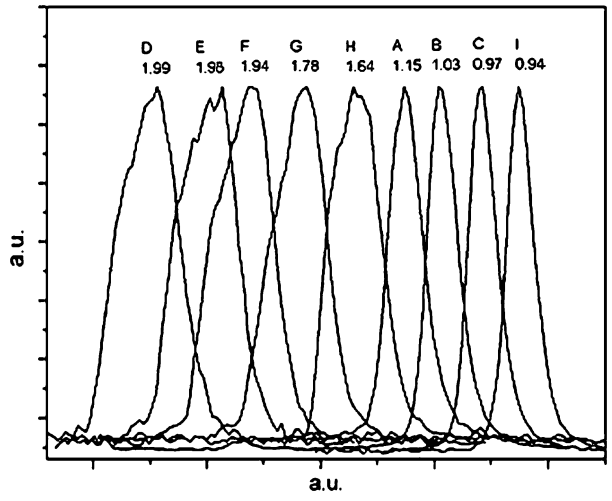

Fig. 3. – Comparison among the different peak width associated with the various analysed zones. The numbers are the peak broadening ($\Delta d/d$) derived from a Gaussian fitting of (200) α(Cu) copper peak. Peak intensity is normalised and the peaks are freely translated along the axis. A.u. (Arbitrary units.)

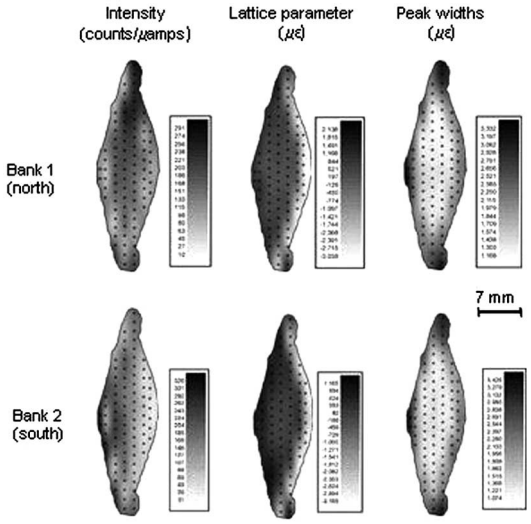

Fig. 4. – Intensity, lattice parameter and peak width distribution maps as derived from the scanning of a cross-section of the sword for the two detectors banks.

separately manufactured since, in the contrary case, an annealing of the antennas would have caused an annealing in the handle too. The three analysed zones in the central body of the sword (sites A, B, C) provide similar peak widths among them, however the peak of zone A (where the blade contribution dominates) is slightly broader according to a possible relatively higher hardening of the tip of the sword.

3˙3. *Cross-section mapping.* – ENGIN-X has been used to scan a cross-section of the sword (see the line in fig. 1). Both the blade and the scabbard were simultaneously scanned. The gauge volume was $1 \times 1 \times 13$ mm^3. From a single peak fitting of the four most intensive reflections (111, 200, 220, 311), the total intensity, lattice parameter variation and average peak width were calculated. Two microstrain maps were hence produced from lattice parameter variation ($\mu\varepsilon = \Delta a/a \times 10^{-6}$) and peak width variation ($\mu\varepsilon = \Delta d/d \times 10^{-6}$). Figure 4 displays the maps provided by the two banks.

The intensity maps, which provide information about the distribution of metal density, are different for the two banks. This is due to absorption phenomena associated with long paths inside the metal. The present resolution is able to give just a vague idea of intensity differences produced by mineralisation distribution. The variation of the lattice parameter in the two sides of the scabbard evidences that the two sheets are composed by a different alloy. The minimum value is $a = 3.663$ Å (8.4 wt% of tin) and the maximum is $a = 3.679$ Å (11.1 wt% of tin). Such a variation is too pronounced to be attributed to residual stresses associated with different hardening degrees of the two parts. This difference was not detected with ROTAX because in that case the main contribution to the diffraction pattern was due to the blade. As shown by the peak width distribution map (fig. 4), the elastic strain in the scabbard is higher in comparison to the bulk of the blade. The present distribution of this latter is compatible with the presence of microstrains along its edge. The cold join of the two sheets composing the scabbard causes a broadening of peak widths because superposition of several microstrain directions.

4. – Conclusions

In this paper we reported an example application of TOF-ND for the non-destructive characterisation of a Villanovan sword. Information about the alloy composition and manufacturing techniques have been successfully achieved using the diffractometers ROTAX and ENGIN-X at ISIS. In particular, the 2D mapping of a cross-section provided by this latter allowed insights on composition and residual stresses of the blade and of the scabbard by exploiting the powerful spatial resolution possibilities of the instrument. Combining phase and peak shape analyses we derived the sword was crafted by cold joining of seven pieces with at least four different compositions, preliminarily produced through independent material processing. The variable composition indicates the craftsman was assembling parts produced in different times, which could suggest a sort of "industrial" manufacturing where a certain quantity of the single piece was separately produced. Unfortunately, this hypothesis cannot be easily demonstrated since the present sword is a unique artefact of Marches' Villanovan and Picenan collections. Some similar objects, found in southern *Etruria*, could provide comparison possibilities in future investigations.

REFERENCES

[1] Kockelmann W., Pantos E. and Kirfel A., in *Radiation in Art and Archaeometry*, edited by Creagh D. C. and Bradley D. (Elsevier, Amsterdam) 2000, pp. 347-377.
[2] Kockelmann W., Kirfel A. and Haenel E., *J. Arch. Sci.*, **28** (2001) 213.
[3] Siano S., Kockelmann W., Zoppi M., Miccio M., Iozzo M., Bafile U., Salimbeni R., Pini R., Celli M. and Moze O., *Appl. Phys. A*, **74** (2002) 1139.
[4] Siano S., Bartoli L., Zoppi M., Kockelmann W., Daymond M., Dann J., Garagnani G. and Miccio M., in *Proceedings of the International Conference "Archaeometallurgy in Europe"*, Vol. **2** (Associazione Italiana di Metallurgia, Milano) 2003, pp. 319-329.
[5] Siano S., Bartoli L., Kockelmann W., Zoppi M. and Miccio M., *Physica B*, **350** (2004) 123.
[6] Siano S., Bartoli L., Santisteban J. R., Kockelmann W., Daymond M., Miccio M. and De Marinis G., *Archaeometry*, **48** (2006) 77.
[7] Pantos E., Kockelmann W., Chapon L. C., Lutterotti L., Bennet S. L., Tobin M. J., Mosselmans J. F. W., Pradell T., Salvado N., Butì S., Garner R. and Prag A. J. N. W., *Nucl. Instrum. Methods B*, **239** (2005) 16.
[8] Artioli G., Dugnani M., Hansen T., Lutterotti L., Pedrotti A. and Sperl G., in *Die Gletschermumie aus der Kupferzeit 2*, edited by Fleckinger A. (Museo archeologico dell'Alto Adige, Bolzano) 2003, pp. 9-22.
[9] Coppola R., Lapp A., Magnani M. and Valli M., *Appl. Phys. A*, **74** (2002) 1066.
[10] Larson A. C. and Von Dreele R. B. in Report LAUR86-748, Los Alamos National Laboratory, New Mexico (1986).
[11] Dann J. A., Daymond M. R., Edwards L., James J. and Santisteban J. R., *Physica B*, **350** (2004) 511.
[12] Scott D. A., in *Metallography and microstructure of ancient and historic metals* (The Getty Conservation Institute, Los Angeles) 1991, pp. 23-24.